High-density microfluidic arrays for cell cytotoxicity analysis†

Zhanhui Wang,[ab] Min-Cheol Kim,[a] Manuel Marquez[cde] and Todd Thorsen*[a]

Received 22nd December 2006, Accepted 13th March 2007
First published as an Advance Article on the web 4th April 2007
DOI: 10.1039/b618734j

In this paper, we report on the development of a multilayer elastomeric microfluidic array platform for the high-throughput cell cytotoxicity screening of mammalian cell lines. Microfluidic channels in the platform for cell seeding are orthogonal to channels for toxin exposure, and within each channel intersection is a circular chamber with cell-trapping sieves. Integrated, pneumatically-actuated elastomeric valves within the device isolate the microchannel array within the device into parallel rows and columns for cell seeding and toxin exposure. As a demonstration of the multiplexing capability of the platform, a microfluidic array containing 576 chambers was used to screen three cell types (BALB/3T3, HeLa, and bovine endothelial cells) against a panel of five toxins (digitonin, saponin, $CoCl_2$, $NiCl_2$, acrolein). Evaluation of on-chip cell morphology and viability was carried out using fluorescence microscopy, with outcomes comparable to microtiter plate cytotoxicity assays. Using this scalable platform, cell seeding and toxin exposure can be carried out within a single microfluidic device in a multiplexed format, enabling high-density parallel cytotoxicity screening while minimizing reagent consumption.

Introduction

High-throughput cell-based screening platforms have stimulated tremendous interest in the pharmaceutical industry for improved high-throughput cell-based screening platforms to expedite target validation as well as for use in pre-clinical trials.[1] However, current methods to perform cell-based drug screening assays are generally expensive and labor-intensive, utilizing high-density multi-well plates or array bioreactors that are operated using cumbersome manual or expensive robotics-based operations.[2] Consequently, developing a technology that can perform such experiments in a cheaper, easier, and high-throughput manner will have a major impact on a number of fields, ranging from drug discovery to tissue engineering.

Recently, microfabrication and microfluidic technologies have been recognized as potential platforms for cell-based biosensing and drug screening.[3] Unlike high-density microplate systems, microfluidic networks, consisting of micromachined or molded channels with micron dimensions, have the capability to perform experiments in a high-throughput manner in nanolitre or picolitre volumes[4] using integrated components such as valves, pumps and gradient generators. In recent years, microfluidics has been applied to several cell-based biological applications including mammalian cell patterning,[5–8] monitoring cellular responses to chemical gradients,[9,10] cellular differentiation,[11] and dynamic gene expression.[12,13] Khademhosseini *et al.* recently described a multiplexed soft lithographic method to fabricate multi-phenotype cell arrays for drug screening.[14] However, separate microfluidic devices were utilized for cell seeding and drug exposure.

A practical microfluidic cell array for cytotoxicity screening ideally requires uniform cell loading and distribution in each chamber. Small perturbations to fluid flow can significantly disturb cell positions in microculture chambers with nanolitre volumes,[15] exacerbating cell clumping and local exhaustion of nutrients in the growth media that adversely stress the cell culture even without toxin exposure. To address this challenge, several groups developed a number of microfluidic techniques to confine cells in defined positions,[14–25] including U-shaped weirs,[22–24] poly(dimethylsiloxane) (PDMS) wells,[14] C-shaped rings with microsieves,[15] holographic optical traps,[25] and dielectrophoresis.[18]

In this report, we describe the development of a microfluidic array platform for high-throughput cell cytotoxicity screening. The channels in this platform are individually addressable in both directions (column and row). The channels for cells seeding are orthogonal to channels for toxins exposure, and within each channel intersection is a circular chamber that can be compartmentalized by integrated pneumatically-actuated elastomeric valves. Several U-shaped micro cell sieves are fabricated within each culture chamber to form several low flow velocity regions, creating a uniform distribution of small seed populations of cells ($\sim$10 cells per sieve) to promote cell–cell stimulation and the growth of healthy monolayers under microculture conditions.

[a]*Department of Mechanical Engineering, Massachusetts Institute of Technology, Cambridge, MA, 02139, USA. E-mail: thorsen@mit.edu*
[b]*INEST Group Postgraduate Program, Philip Morris USA, Richmond, VA, 23234, USA*
[c]*NIST Center for Theoretical and Computational Nanosciences, Gaithersburg, MD, 20899, USA*
[d]*Harrington Department Bioengineering Arizona State University, Tempe, AZ, 85287, USA*
[e]*Research Center, Philip Morris USA, 4201 Commerce Road, Richmond, VA, 23234, USA*
† This paper is part of a special issue 'Cell and Tissue Engineering in Microsystems' with guest editors Sangeeta Bhatia (MIT) and Christopher Chen (University of Pennsylvania).

Experimental

Microfluidic array fabrication

The microfluidic device was fabricated in PDMS (Sylgard 184, Dow Corning) by multilayer soft lithography.[26,27] Two photoresist-based molds were used to fabricate the multilayer device, corresponding to flow and control layers patterned with respective microchannel structures. Using standard lithographic procedures, AZXT50 positive photoresist (AZ Electronic Materials USA Corp.) was patterned onto separate silicon wafers using high-resolution design transparencies to create the distinct positive relief molds. To promote complete valve closure in the assembled devices, the channel profiles were rounded on the flow layer mold by placing the wafer on a hotplate at 150 °C for one minute to reflow the photoresist. The post-baked molds were then treated with chlorotrimethylsilane (Aldrich) to facilitate the release of the elastomer after molding. Consecutive replica molding from the microfabricated masters and chemical bonding steps were used to create three-layer elastomeric devices. To fabricate the devices, liquid silicone elastomer (Dow Corning Sylgard 184 mixed in a ratio of 5 : 1 part A : B) was poured on the control mold to a thickness of 5 mm, and baked at 80 °C for 20 min, while elastomer (20 : 1 part A : B) was spin coated onto the flow master (2000 rpm for 60 s) and baked for 80 °C for 18 min. The partially cured thick layer was peeled from the master and aligned over the flow mold under a microscope. The two-layer structure was then baked for 20 min, chemically cross-linking the two layers into a single structure. The bonded flow and control layers were then peeled from the flow master, access ports were punched using a 23 gauge luer stub (BD Biosciences) at both flow and control layers. The microchannel surface containing the exposed flow channels and connection ports were thoroughly cleaned using isopropanol, blown dry with nitrogen, and irreversibly bonded to a glass slide assisted by oxygen plasma surface treatment (150 mTorr, 50 W, 20 s).

In the final assembled devices, the flow channels are 40 μm (h) × 100 μm (w) with a circular chamber at each channel intersection (diameter 400 μm), while the control channels are 40 μm (h) × 200 μm (w) in the control valving regions, and 30 μm (w) where they cross over flow lines and valve closure is not desired. Within the circular chambers in the flow layer are eight PDMS U-shaped cell sieves. Each sieve is semicircular, 80 μm (d), 20 μm (w), and 40 μm (h) (equivalent to the flow layer height), with two apertures (8 μm). The thin PDMS membrane separating a control channel crossing over a flow channel constitutes a valve; when the pressure in the control channel is high, the silicone membrane is deflected downward, and the flow channels are closed. Where control channels are narrow, they can cross flow channels without interrupting flow at the valve actuation pressure as higher pressures are necessary to deflect membranes with smaller surface areas.

Off-chip control of the valves, pressurized by a nitrogen source gated by miniature solenoid check valves (The Lee Co.), was carried out using an analog-to-digital logic board (National Instruments PCI-DIO-32HS) driven by Java-based code.[28] The control channels were initially filled with water to prevent diffusion of air bubbles through the PDMS membrane into the flow layer and evaporation during cell culture. Selectively applying pressure (15 psi) to the water-filled control channels toggles the valves between the open and closed states.

Microfluidic simulations for sieve optimization

Optimization of the geometry and positioning of the cells sieves in a single microchamber was achieved by simulating the cell loading process. Computational fluid dynamics (CFD) simulations were carried out using a commercial CFD tool (STAR-CD 3.15a, CD-adpaco), which is based on the finite volume method (FVM). Momentum equations and the continuity equation were solved using the SIMPLE (Semi-Implicit Method for Pressure Linked Equation) algorithm.

Within the simulation, the transient motion of every cell was calculated by using a one-way coupled Lagrangian approach for the pre-computed Newtonian flow fields. This method includes spatial interpolation of the flow velocity at the position of each cell center. Each cell was assumed to be a solid sphere with a hydraulic diameter of 10 μm, and the forces considered in the equation of motion were the Stokes drag, the pressure gradient, diffusive and buoyant forces, and a spring force to model the elastic collision between cells.[29] The cell trajectory code was validated against the experimental results of the annular expansion channel.[30,31] A fourth-order Rosenbrock method based on an adaptive time-stepping technique was utilized as the integration method, as it is more reliable for stringent parameters than the Runge–Kutta method.[32]

Cell culture

BALB/3T3 murine embryonic fibroblast and HeLa cell lines were purchased from Advanced Type Culture Collection (ATCC), and cell culture reagents were purchased from Gibco Invitrogen Corp. The bovine endothelial cells were a kind gift from Prof. Forbes Dewey, MIT. All cell lines were manipulated under sterile tissue culture hoods and maintained in a 5% CO_2 humidified incubator at 37 °C. The BALB/3T3 line was maintained in Dulbecco modified Eagle medium (DMEM) supplemented with 10% fetal bovine serum (FBS). The HeLa line was maintained in Eagle mimimum essential medium (MEM)/10% FBS. Endothelial cells were maintained in DMEM/10% FBS. Once the cells were confluent, they were trypsinized (0.25% in EDTA, Sigma) and passaged at a 1 : 5 sub-culture ratio.

Microfluidic device cell seeding

The microfluidic devices were autoclaved, rinsed with 1x phosphate-buffered saline, pH 7.4 (PBS), and degassed by driving trapped air through the walls of the gas-permeable device. The flow channels glass surface was pre-coated with 20 mg mL^{-1} gelatin (Sigma) for 1 hour to promote cells attachment. Excess gelatin was removed by rinsing with 1x PBS. A haemocytometer was used to assess the culture density of each sub-cultured cell type (48 hours after passage). After counting, all cell types were spun down in a centrifuge (1000 rpm, 5 minutes) and reconstituted at 10^6 cells ml^{-1} in DMEM/10% FBS. To load the cells into the circular cell

Table 1 Comparative cell cytotoxicity: microfluidic array *vs.* 96 well tissue culture plate

	Microfluidic array			96 Well culture plate		
% Viability (S.D.)	HeLa	BALB/3T3	Bov. endo.	HeLa	BALB/3T3	Bov. endo.
PBS	99.3 ± 0.8	100	98.8 ± 1.1	100	100	99.6 ± 0.6
Dig(H)	0	0	0	0	0	0
Dig(L)	69.4 ± 2.3	69.9 ± 2.9	71.1 ± 2.3	73.7 ± 1.2	73.0 ± 2.6	70.7 ± 3.8
Sap(H)	0	0	0	0	0	0
Sap(L)	74.5 ± 2.4	77.8 ± 5.1	80.4 ± 2.0	75.7 ± 2.1	80.3 ± 1.5	76.3 ± 3.5
$CoCl_2$(H)	80.8 ± 4.4	80.4 ± 3.3	82.5 ± 3.9	85.6 ± 2.6	83.3 ± 2.8	80.6 ± 1.6
$CoCl_2$(L)	89.3 ± 3.4	89.4 ± 1.7	88.9 ± 2.9	91.0 ± 2.2	87.7 ± 2.1	90.0 ± 2.2
$NiCl_2$(H)	80.1 ± 3.5	80.6 ± 3.1	78.8 ± 5.4	80.6 ± 1.7	81.6 ± 2.0	82.3 ± 2.0
$NiCl_2$(L)	88.3 ± 5.3	91.0 ± 2.8	89.4 ± 2.5	89.3 ± 2.5	92.3 ± 2.1	89.6 ± 4.1
Acrol(H)	0	0	0	0	0	0
Acrol(L)	84.9 ± 3.8	85.4 ± 3.0	83.3 ± 3.1	82.3 ± 1.5	84.7 ± 1.6	85.0 ± 3.5

culture chambers, a vertical array valve was actuated, each cell line ($\sim 10^6$ cells mL^{-1}, 1 μl min^{-1} volumetric flow rate, 3 min total load time) was injected into the device through the inlets using a 24-channel roller pump (ISMATEC), and the cells were incubated statically at 37 °C/5% CO_2 for 24 h. 12 hours into the incubation, the roller pump was used to change out the media, replenishing critical metabolites and removing potentially toxic waste products.

Cell toxin exposure and analysis

After cell seeding, the cells within the microfluidic arrays were exposed to a panel of toxins (digitonin, saponin, $CoCl_2$, $NiCl_2$, acrolein), using 1x PBS, pH 7.4 as a toxin-free control. Working solutions of the toxins were diluted in 1x PBS: (0.003 and 0.1% (w/w) digitonin, 0.01% and 0.1% (w/w) saponin, 4.2 and 42 mM $CoCl_2(6H_2O)$, 4.2 and 42 mM $NiCl_2(6H_2O)$). Acrolein (0.02 and 0.5 mM) was diluted in DMEM/10% fetal calf serum, as a longer exposure time was necessary to observe any cytotoxocity, requiring the presence of growth media. Activating the vertical array valve, the working solutions (with the exception of acrolein) were flowed across the seeded cells at a rate of 0.5 μl min^{-1} with the 24-channel roller pump (ISMATEC) for a period of one hour at room temperature (RT) (25 °C). For the acrolein solution, a 10 hour static exposure was carried out at 37 °C, 5% CO_2 after the initial 25 °C RT incubation. Post-exposure, the cells were washed in 1x PBS and stained with LIVE/DEAD viability solution (calcein AM and ethidium homodimer-1) (Invitrogen). Calcein AM is a fluorogenic esterase substrate that is hydrolyzed intracellularly to a green fluorescent product (calcein); thus green fluorescence is an indicator of live cells. Ethidium homodimer-1 is a high-affinity, red fluorescent nucleic acid stain that is only able to pass through the compromised membranes of dead cells. Subsesquent visualization and digital live/dead analysis of the stained cells was carried out using an inverted fluorescent microscope (Nikon TE2000-U, 10x Plan Apo) equipped with a cooled CCD camera for image capture (Apogee Instruments KX32ME, 1 s exposure). The fluorescent microscope images of cells exposed to toxins are shown in Fig. 4 (Results and Discussion). Control parallel toxin exposure experiments were performed by seeding BALB/3T3, HeLa and bovine endothelial cells ($\sim 10^6$ ml^{-1} in DMEM/10% FBS) into 96-well tissue culture dishes (VWR), 100 μl culture medium per well, under the same incubation and exposure times as the microfluidic array, with comparative viability results reported in Table 1.

Results and discussion

A microfluidic array platform was designed to fabricate multiplexed live cell arrays for cell cytotoxicity screening (Fig. 1). Operating the array to seed the chambers and subsequently expose them to the toxin panel is simply achieved using integrated elastomeric vertical and horizontal array valves, respectively, under LabView control. When the vertical array valve is actuated (horizontal valve array open), the microchannels in the 'column' direction are individually isolated and various cell lines or primary cultures can be delivered simultaneously into the series of interconnected microchambers in each column. Eight U-shaped sieves within each chamber promote uniform cell seeding across chambers. Likewise, actuating the horizontal array valve (vertical valve array open) results in the parallel exposure of cell cultures seeded in the chambers to the panel of toxins.

A significant challenge in the development of microfluidic devices for cell culture-based applications is providing a local environment conducive to metabolite exchange and proliferation. While microscale devices have proven to be useful tools for the trapping and assaying of single cells,[17–19,21–24] especially for molecular analysis, starting a healthy cell culture *in vitro* often requires a critical cell density. Cell–cell interaction and local cytokines provide local stimuli critical for

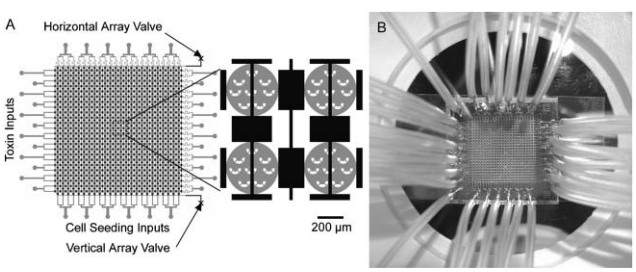

Fig. 1 (A) Schematic of the 24 × 24 chamber microfluidic cytotoxicity array. Each chamber contains eight micro cell sieves for cell trapping. Each sieve is semicircular with an outer diameter of 80 μm, 40 μm (h), 15 μm (w), with two apertures (8 μm width). (B) Image of the microfluidic cytotoxicity array chip with fluid interconnects.

growth and development, especially in co-culture environments.[33,34] However, achieving uniform cell distribution and proper seeding density within an array of microchambers is difficult, as the flow field within individual chambers is constantly changing as cells begin to aggregate during the seeding process.

To address the cell seeding challenge, CFD was implemented as a design tool to create a cluster of eight U-shaped cell sieves within microchamber, optimizing the geometry to trap a small number of cells per sieve ($\sim$10–15) during cell loading. During the modeling process, a number of U-shaped sieve designs were considered, varying aspect ratio, the number of apertures and the position of each sieve to obtain the requisite number of cells per sieve while minimizing sieve–sieve capture variation. The fluid velocity was simulated as described in the Experimental for a cell chamber geometry containing eight cell sieves. The velocity profile through the single cell chamber with the optimized sieve geometry and layout is shown in Fig. 2A. The fluid velocities in the regions in the cell sieves are reduced, and eight low fluid velocity regions are formed in the cell chamber. Two 8 μm apertures with each cell sieve permit fluid flow through the sieve. As the cells aggregate within the sieves, they block the drainage through the apertures, creating flow resistance that deflects cells into the downstream chambers.

Simulations of cell loading within a single chamber (10^6 cells ml^{-1}) illustrates the capture of cells in the U-shaped sieve arrays (Fig. 2B). Experimental validation of the model was carried out using the HeLa and BALB/3T3 cell lines, loading eight columns of the microfluidic array (10^6 cells ml^{-1} in the growth media of each cell line) at a volumetric flow rate of 1 μL min^{-1} for 3 min. Cells confined within the sieves of the respective chambers (192 chambers in total for each cell type) were counted manually using an inverted light microscope (Nikon TE2000-U, 10× plan objective, NA 0.25). Cell loading within the individual sieves of the microfluidic array was quite uniform, with an average cell number per sieve of 11.2 ± 1.4 cells per sieve (HeLa) and 11.5 ± 2.4 cells per sieve (BALB/3T3)), in comparison to 15.2 ± 0.72 cells per sieve for the theoretical simulation. The variation in cell number per sieve across different chambers of a column was statistically insignificant. A visual comparison of

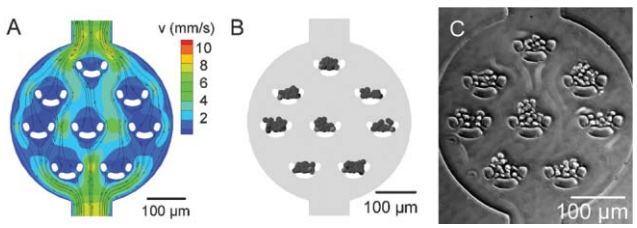

Fig. 2 (A) Theoretical flow velocity profile through single chamber with eight cell sieves. Velocity in the cell sieve is significantly reduced compared to outside the sieve, and eight low flow velocity regions are formed within the chamber. (B) Simulation results for cell capture based on an input cell density of 10^6 cells ml^{-1}, a flow rate of 1 μl min^{-1} through the chamber, and a total flow time of 3 min. (C) Comparative experimental cell capture results using HeLa cells, with flow and cell density parameters matching those used in simulation.

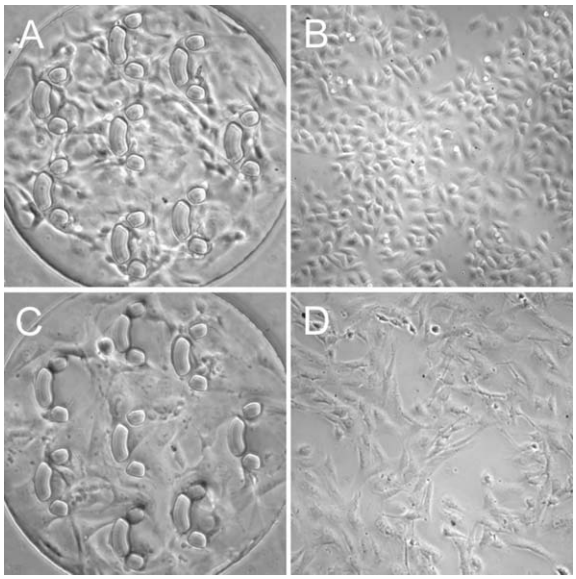

Fig. 3 Cells morphology, comparing cells cultured for 24 hours in the microfluidic array chambers (left) *vs.* a 96 well tissue culture plate (right); HeLa cells (A,B), BALB/3T3 cells (C,D).

the theoretical *vs.* experimental distribution in a single chamber using HeLa cells is shown in Fig. 2B,C. The lower experimental trapped numbers can be potentially attributed to several factors not included in the model, including individual cell size variation and small cell clumps (2–3 cells) in the cell suspension loaded into the chip. The model is also based on a single chamber, limited by the computational time to run the simulation, while the experimental device contains 24 chambers. While the pressure drop per chamber is low ($\sim$17 Pa by simulation), the coupling of the large number of chambers in series is likely to induce small changes in local flow field around the individual sieves.

Image captures of the HeLa and 3T3 after 24 hour culture within the seeded microchambers show good adhesion and morphology, comparable to control experiments in which cells were cultured in 96 well plates (10^6 ml^{-1}, 100 μl growth media per well) (Fig. 3). After 24 hours in culture, spreading of the HeLa and 3T3 cells out of the sieves within the microchambers was observed, consistent with the cell migration rates ($\sim$10 μm h^{-1}) of adherent cells like BALB/3T3 observed *in vitro* within tissue culture flasks.[35] No necrosis or rounding up of the cells was observed in either the microchambers or the plates.

To apply the microfluidic array to cell cytotoxicity screening, a matrix was set up consisting of three cell types (HeLa, BALB/3T3, bovine endothelial) and low (L) and high (H) concentrations (see Experimental) of five toxins: saponin, digitonin, $CoCl_2$, $NiCl_2$, and acrolein. The cells were initially cultured in the devices for 24 hours at 37°C/5% CO_2. After cell seeding, the microchambers were flushed with 1x PBS, followed by the addition of the toxins loaded in individual rows of the device using a 24-channel roller pump. A parallel experiment was carried out in 96 well culture microplates using the identical growth and culture conditions for comparison. After toxin exposure, the microchambers were promptly rinsed

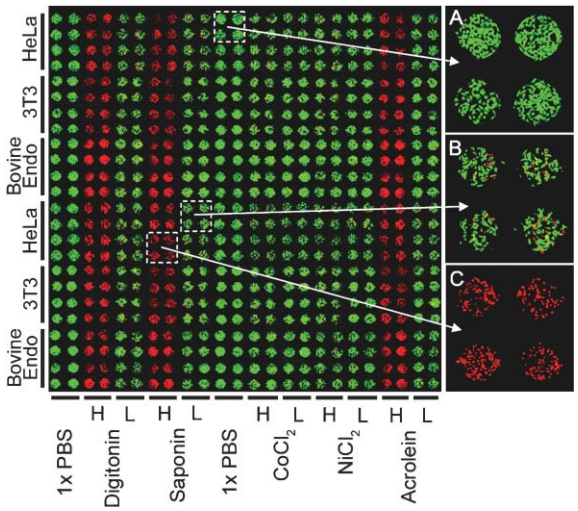

Fig. 4 Composite image of microfluidic cytotoxicity array chip after toxin challenge and live/dead staining. (H) and (L) notations on the *x*-axis represent high and low concentrations for each toxin. Inset (A): HeLa cells challenged with 1x PBS control. (B) HeLa cells challenged with low dose of saponin (0.01% w/w in 1x PBS). (C) HeLa cells challenged with high dose of saponin (0.1% w/w in 1x PBS).

with 1x PBS, the cells were stained with LIVE/DEAD stain (Molecular Probes), and the chip was visualized using fluorescent microscopy. A cooled CCD camera (Apogee Instruments) was used to capture images of individual chambers within the microarray for subsequent viability analysis. A composite image of the stained chip is shown in Fig. 4. From the image, some chamber–chamber growth variation can be seen. However, the live/dead cytotoxicity data was comparable across different chambers in terms of mean percent viability for each individual cell type/toxin combination, with most standard deviation values <4%. Moreover, the viability data in the microfluidic array was comparable to the data obtained from the parallel experiments carried out in the 96 well culture plates in terms of viability and chamber–chamber variation (Table 1).

Cytotoxicity responses in the microfluidic array varied according to toxin type and concentration. Saponins, high molecular weight glycosides, which include digitonin, cause poration of eukaryotic cell membranes and cytotoxicity at high concentrations. At 0.1% w/w concentrations, 100% cell death in all cultures (microarray and plate) was observed with both saponin and digitonin treatment, while lower concentrations of the two toxins (0.01% and 0.003%, respectively) resulted in post-exposure cell viability rates between 70 and 80%. Metal chlorides like $NiCl_2$ and $CoCl_2$ have been associated with the apoptosis and necrosis of endothelial cells through damage to the cytoskeletal matrix and DNA damage through free radical generation.[36] After a one hour exposure time to the high (42 mM) and low (4.2 mM) concentrations of the metal salts, average viability rates of ~80 and 90% were observed for all cell lines. The high viability of the metal-salt exposed cultures is not surprising given the short toxin exposure time (1 h), as water-soluble metal ions are only taken up slowly by cells.[37] Acrolein, an environmental toxin, primarily slows down cell proliferation by reducing cellular glutathione levels (GSH).[38] While toxic at sub-micromolar levels, cell stress and death, triggered by the generation on peroxide and superoxide radicals at concentrations greater that 100 μm,[39] requires prolonged exposure to acrolein (several hours). Accordingly, the acrolein exposure was carried out in growth media (DMEM/10% serum) to prevent cell starvation and the exposure time was extended 10 h at 37 °C/5% CO_2. Post-exposure, cells treated with the low dose of acrolein (0.02 mM) had viability rates of 80–85% while the high dose groups (0.5 mM) resulted in 100% cell death.

Multiplexed microfluidic array devices for cell biology, like the cytotoxicity-screening chip described in this manuscript, are valuable tools that have the potential to be applied to a variety of real-time assays that are very difficult to carry out in multi-well plate format. High-density endpoint screens, like cytotoxicity or immunoassays, can certainly be scaled up in high-density microtiter plates (using robotic automation and 1584 well plates, for example). However, the ability to carry out simple dynamic experiments, like a spatiotemporal cell response to a chemical stimulus, is extremely difficult to carry out in plate format, as factors such as pipetting errors, mixing, and time-to-analysis introduce assay-to-assay variations that adversely affect reproducibility. In contrast, microfluidics offers a level of assay control previously unattainable at the macroscale, providing the benchtop researcher with a tool to not only precisely manipulate and position cells in a low-cost, parallel format, but also to carry out sophisticated operations at the fluid level. Examples include chemical gradient generation for chemotaxis[40,41] and the delivery of biochemical stimulation agents to confined cells in defined pulses.[42]

Conclusions

This paper describes the development of a PDMS microfluidic array device containing micro cell sieves for cell cytoxicity screening. Fabricated using multilayer soft lithography, the screening of three cell lines against two concentrations of five toxins was demonstrated within the 24 × 24 array. Relatively high cell uniformity per microchamber was achieved using eight microfabricated cell sieves within each chamber, and CFD as a tool to optimize the placement and geometry of the individual sieves. Good adhesion and spreading of each of the adherent cell lines was observed in the microfluidic array devices, comparable to cells grown in 96 well tissue culture plates. Likewise, a comparison of the cytotoxicity data (microarray *vs.* 96 well plate) exhibited a high degree of correlation, with most direct mean viability percentages for a given cell type/toxin concentration within 1–2%. While the microfluidic array was designed as a simple cytotoxicity tool, we anticipate that it could be used for even more sophisticated cell-based assays, including the defined patterning of multiple cell types/chamber and spatiotemporal drug response assays.

Acknowledgements

This work was partially supported through an INEST grant from Philip Morris USA and a Korean Research Foundation Grant (KRF-2006-D00019).

References

1 S. A. Sundberg, *Curr. Opin. Biotechnol.*, 2000, **11**, 47–53.
2 S. B. Chen, Q. S. Zhang, X. Wu, P. G. Schultz and S. Ding, *J. Am. Chem. Soc.*, 2004, **126**, 410–411.
3 T. H. Park and M. L. Shuler, *Biotechnol. Prog.*, 2003, **19**, 243–253.
4 R. M. McCormick, R. J. Nelson, M. G. Alonso-Amigo, D. J. Benvegnu and H. H. Hooper, *Anal. Chem.*, 1997, **69**, 2626–2630.
5 D. T. Chiu, N. L. Jeon, S. Huang, R. S. Kane, C. J. Wargo, I. S. Choi, D. E. Ingber and G. M. Whitesides, *Proc. Natl. Acad. Sci. U. S. A.*, 2000, **97**, 2408–2413.
6 Y. L. Mi, Y. N. Chan, D. Trau, P. B. Huang and E. Q. Chen, *Polymer*, 2006, **47**, 5124–5130.
7 S. W. Rhee, A. M. Taylor, C. H. Tu, D. H. Cribbs, C. W. Cotman and N. L. Jeon, *Lab Chip*, 2005, **5**, 102–107.
8 W. Tan and T. A. Desai, *Tissue Eng.*, 2003, **9**, 255–267.
9 N. L. Jeon, H. Baskaran, S. K. Dertinger, G. M. Whitesides, L. Van de Water and M. Toner, *Nat. Biotechnol.*, 2002, **20**, 826–830.
10 P. J. Hung, P. J. Lee, P. Sabounchi, R. Lin and L. P. Lee, *Biotechnol. Bioeng.*, 2005, **89**, 1–8.
11 A. Tourovskaia, X. Figueroa-Masot and A. Folch, *Lab Chip*, 2005, **5**, 14–19.
12 D. Thompson, K. R. King, K. J. Wieder, M. Toner, M. L. Yarmush and A. Jayaraman, *Anal. Chem.*, 2004, **76**, 4098–4103.
13 K. R. King, S. Wang, D. Irimia, A. Jayaraman, M. Toner and M. L. Yarmush, *Lab Chip*, 2007, **7**, 77–85.
14 A. Khademhosseini, J. Yeh, G. Eng, J. Karp, H. Kaji, J. Borenstein, O. C. Farokhzad and R. Langer, *Lab Chip*, 2005, **5**, 1380–1386.
15 P. J. Lee, P. J. Hung, V. M. Rao and L. P. Lee, *Biotechnol. Bioeng.*, 2006, **94**, 5–14.
16 A. R. Wheeler, W. R. Throndset, R. J. Whelan, A. M. Leach, R. N. Zare, Y. H. Liao, K. Farrell, I. D. Manger and A. Daridon, *Anal. Chem.*, 2003, **75**, 3581–3586.
17 M. S. Yang, C. W. Li and J. Yang, *Anal. Chem.*, 2002, **74**, 3991–4001.
18 J. Voldman, M. L. Gray, M. Toner and M. A. Schmidt, *Anal. Chem.*, 2002, **74**, 3984–3990.
19 X. Y. Peng and P. C. H. Li, *Anal. Chem.*, 2004, **76**, 5273–5281.
20 U. Seger, S. Gawad, R. Johann, A. Bertsch and P. Renaud, *Lab Chip*, 2004, **4**, 148–151.
21 H. K. Wu, A. Wheeler and R. N. Zare, *Proc. Natl. Acad. Sci. U. S. A.*, 2004, **101**, 12809–12813.
22 P. C. H. Li, L. de Camprieu, J. Cai and M. Sangar, *Lab Chip*, 2004, **4**, 174–180.
23 X. J. Li and P. C. H. Li, *Anal. Chem.*, 2005, **77**, 4315–4322.
24 D. Di Carlo, N. Aghdam and L. P. Lee, *Anal. Chem.*, 2006, **78**, 4925–4930.
25 K. C. Neuman, E. H. Chadd, G. F. Liou, K. Bergman and S. M. Block, *Biophys. J.*, 1999, **77**, 2856–2863.
26 M. A. Unger, H.-P. Chou, T. Thorsen, A. Scherer and S. R. Quake, *Science*, 2000, **288**, 113–116.
27 V. Studer, G. Hang, A. Pandolfi, M. Ortiz, W. F. Anderson and S. R. Quake, *J. Appl. Phys.*, 2004, **95**, 393–398.
28 J. P. Urbanski, W. Thies, C. Rhodes, S. Amarasinghe and T. Thorsen, *Lab Chip*, 2005, **6**, 96–104.
29 W. A. Lam, M. J. Rosenbluth and D. A. Fletcher, *Blood*, 2007, DOI: 10.1182/blood-2006-08-043570, in press.
30 T. Karino and H. Goldsmith, *Philos. Trans. R. Soc. London, Ser. B*, 1977, **279**, 413–445.
31 M.-C. Kim, J. H. Nam and C.-S. Lee, *Ann. Biomed. Eng.*, 2006, **34**, 958–970.
32 W. H. Press, S. A. Teukolsky, W. T. Vetterling and B. P. Flannery, *Numerical Recipes in C*, Cambridge University Press, Cambridge, 1992.
33 S. N. Bhatia, U. J. Balis, M. L. Yarmush and M. Toner, *Biotechnol. Prog.*, 1998, **14**, 378–387.
34 J. El-Ali, P. K. Sorger and K. F. Jensen, *Nature*, 2006, **442**, 403–411.
35 G. Kumar, J. J. Meng, W. Ip, C. C. Co and C. C. Ho, *Langmuir*, 2005, **21**, 9267–9273.
36 K. Peters, R. E. Unger, S. Barth, T. Gerdes and C. J. Kirkpatrick, *J. Mater. Sci.: Mater. Med.*, 2001, **12**, 955–958.
37 T. Schwerdtle, A. Seidel and A. Hartwig, *Carcinogenesis*, 2002, **23**, 47–53.
38 N. D. Horton, B. M. Mamiya and J. P. Kehrer, *Toxicology*, 1997, **122**, 111–22.
39 C. C. Wu, C. W. Hseih, P. H. Lai, J. B. Lin, Y. C. Lin and B. S. Wung, *Toxicol. Appl. Pharmacol.*, 2006, **214**, 244–52.
40 H. B. Mao, P. S. Cremer and M. D. Manson, *Proc. Natl. Acad. Sci. U. S. A.*, 2003, **100**, 5449–5454.
41 N. L. Jeon, H. Baskaran, S. K. W. Dertinger, G. M. Whitesides, L. Van de Water and M. Toner, *Nat. Biotechnol.*, 2002, **20**, 826–830.
42 P. Sabounchi, C. Ionescu-Zanetti, R. Chen, M. Karandikar, J. Seo and L. P. Lee, *Appl. Phys. Lett.*, 2006(88) Art. No. 183901.